Mechanical Properties of Biodegradable Composites from Poly Lactic Acid (PLA) and Microcrystalline Cellulose (MCC)

Aji P. Mathew,[1] Kristiina Oksman,[1] Mohini Sain[2]

[1]*Department of Engineering Design and Materials, Norwegian University of Science and Technology, Trondheim, Norway*
[2]*Earth Sciences Centre, Faculty of Forestry and Chemical Engineering, University of Toronto, Toronto, Canada*

Received 22 March 2004; accepted 27 October 2004
DOI 10.1002/app.21779
Published online in Wiley InterScience (www.interscience.wiley.com).

ABSTRACT: Biodegradable composites were prepared using microcrystalline cellulose (MCC) as the reinforcement and polylactic acid (PLA) as a matrix. PLA is polyester of lactic acid and MCC is cellulose derived from high quality wood pulp by acid hydrolysis to remove the amorphous regions. The composites were prepared with different MCC contents, up to 25 wt %, and wood flour (WF) and wood pulp (WP) were used as reference materials. Generally, the MCC/PLA composites showed lower mechanical properties compared to the reference materials. The dynamic mechanical thermal analysis (DMTA) showed that the storage modulus was increased with the addition of MCC. The X-ray diffraction (XRD) studies on the materials showed that the composites were less crystalline than the pure components. However, the scanning electron microscopy (SEM) study of materials showed that the MCC was remaining as aggregates of crystalline cellulose fibrils, which explains the poor mechanical properties. Furthermore, the fracture surfaces of MCC composites were indicative of poor adhesion between MCC and the PLA matrix. Biodegradation studies in compost soil at 58°C showed that WF composites have better biodegradability compared to WP and MCC composites. The composite performances are expected to improve by separation of the cellulose aggregates to microfibrils and with improved adhesion. © 2005 Wiley Periodicals, Inc. J Appl Polym Sci 97: 2014–2025, 2005

Key words: bio-composites; microcrystalline cellulose; morphology; dynamic mechanical thermal properties; mechanical properties

INTRODUCTION

Currently, natural fiber reinforced polymer composites technology is focused on creating low cost, high performance, and lightweight materials to replace pure polymers or glass fiber composites. There have been intensive research and product development of composite materials from petroleum based polymers like polypropylene and polyethylene reinforced with natural fibers.[1–5] These composite materials are used extensively in automotive applications, building materials, and household products.[6–8] The advantages of using lignocellulosic fibers as reinforcements in different polymers are reduced weight, relatively good stiffness and strength, as well as low cost and ease of disposal. Composites prepared using jute, flax, banana, sisal, pineapple, coir, oil palm, etc have been studied by several scientists.[9–11] The potential property improvement of any composite material depends on the degree of dispersion and the degree of interaction/adhesion between the matrix and reinforcing phase.[12,13] The effect of processing techniques on the properties of composites was investigated by Mattoso and coworkers, and they concluded that twin screw extrusion resulted in better fiber dispersion with fibers being dissociated to the form of individual ultimatum.[14,15] The use of reinforcements that provide large surface area is considered as a method for obtaining better interaction between the matrix and reinforcement, leading to better mechanical properties, heat resistance, dimensional stability, etc.[16,17]

However, of late, inspired by the growing environmental awareness by all and new standards including "End of Life Vehicle" (ELV) regulations in the EU automotive sector, there is a deliberate interest to look for systems that are even more environmental friendly and biodegradable. Therefore, materials based on raw materials derived from natural resources of plant or animal origin and synthetic polymers with biodegradable backbones are being studied. Biopolymers like soy-oil based epoxy, starch based polymers, polycaprolactone (PCL), polyhydroxy butyrate (PHB), polylactic acid (PLA), and polyester amide have been investigated by scientists as a potential matrix for biodegradable and environmental friendly composites.[18–22] The studies on PLA and especially PLA based com-

Correspondence to: K. Oksman (kristiina.oksman@ntnu.no).

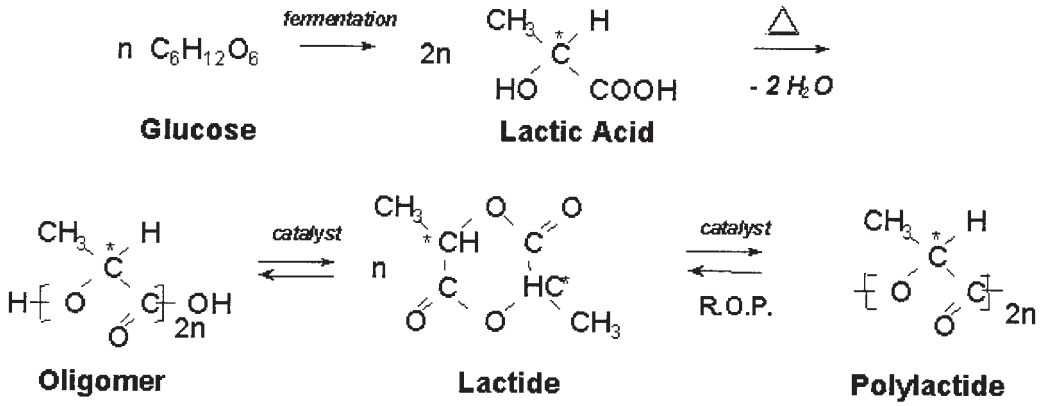

Figure 1 Synthesis and chemical structure of PLA.

posites are very few, and works on natural fiber composites filled PLA is yet to be explored.[23–26] Polylactic acid is a versatile polymer made from renewable agricultural raw materials and is fully biodegradable. Another feature that makes this polymer interesting is the fact that it can be processed similarly to polyolefins; furthermore, PLA owns good stiffness and strength. Polylactic acid (PLA) products are mainly used in applications as plastic bags for household wastes, barriers for sanitary products and diapers, planting, and disposable cups and plates, products with not very high performances. The main drawbacks with PLA properties are low toughness and thermal stability. Therefore, it is interesting to study if the incorporation of reinforcements can improve the toughness and thermal stability. In the present study, PLA based biodegradable composites are prepared with microcrystalline cellulose as the reinforcing phase by twin-screw extrusion followed by injection molding. Our previous study of PLA composites has shown that there is no degradation of PLA during the extrusion process.[26]

Microcrystalline cellulose (MCC), where the amorphous regions are removed by acid hydrolysis, can be a very promising cellulosic reinforcement for polymers. It is basically crystalline cellulose derived from high quality wood pulp, and it is expected to disintegrate into cellulose whiskers after a complete hydrolysis. Native cellulose is one of the strongest and stiffest natural fibers available; the theoretical modulus is estimated at 167.5 GPa,[27] and it has a high potential to act as reinforcing agent in biopolymers. This cellulose fibril can be about 5–10 nm in diameter, and the length varies from 100 nm to several micrometers.[28] MCC has the advantage of high specific surface area compared to other conventional cellulose fibers.

This work was conducted as a preliminary study towards PLA based high performance nano composites using MCC, and we wanted to explore the possibilities of getting MCC dispersed in the PLA matrix as crystalline nanoreinforcements during the extrusion process. Wood flour (WF) and wood pulp (WP) composites were used for comparison. The mechanical properties of the composites were studied, and the morphology of composite fracture surfaces was examined using scanning electron microscopy (SEM). The viscoelastic properties and crystallinity of materials were studied. Further, the biodegradability of the system was looked into by degradation studies in compost soil.

EXPERIMENTS

Methods

Matrix. Poly-L-Lactic Acid, POLLAIT®, was supplied by Fortum Oil and Gas Oy, Porvoo, Finland. The MFI for the PLA is between 1 and 2 g/10 min (190°C, 2.16 kg). The molecular weight (Mw) of the PLA was 97,000g/mol. The synthesis and chemical structure of PLA from glucose is shown in Figure 1.

Reinforcements. The microcrystalline cellulose used as the reinforcement is a powder with a particle size of 10–15 μm. It was supplied by Borregaard Chemcell, Sarpsborg, Norway, and contained $>$ 93% of microcrystalline cellulose. Wood flour (WF) and wood pulp (WP) were used as reference materials. WF (Pine 4–2) was supplied by Scandinavian Wood Fiber AB, Orsa, Sweden, and WP (Terracel^{TM}) was obtained from Rayonier, USA. The physical and chemical characteristics of all three reinforcements and the PLA matrix are summarized in Table I.

Processing

The composite materials were compounded using a twin-screw extruder (Coperion Werner and Pfleiderer ZSK 25 WLE) with a side feeder and gravimetric feeding systems for both main and side feeders. The processing parameters for extrusion are already described

TABLE I
Characteristics of the Used Raw Materials

	PLA	MCC	WP	WF
Density (g/cm^3)	1.26	~0.13–0.25	~0.3–0.4	0.5
pH		5.0–7.0	5.5–8.0	5.0–8.0
Appearance	Transparent pale, pellets	White, free flowing powder	White, fibrous pellets	Pale, coarse powder
Particle size	—	10–15 μm	20–30 μm	150–750 μm
Toxicity	No	No	No	No

in our earlier work on PLA composites.[26] Composites were pelletized for further injection molding. Test samples were injection molded according to the ISO 294 standard for thermoplastics using a Cincinnati ACT Milacron 50 injection molding machine. The injection molding was carried out at 200°C with a velocity of 60mm/s. The mold temperature was kept at 50°C, and the pack pressure was 400 bars. A cooling time of 15 s was given before demolding the test samples. No process aids or other additives were used. The compositions of the composites prepared are given in Table II.

Scanning Electron Microscopy

The morphology of used fibers, MCC, WF, and WP, as well as composite microstructure was studied using a scanning electron microscope (SEM), Cambridge 360. The sample surfaces were sputter coated with Au to avoid charging.

Mechanical testing

The mechanical properties of composites were measured using an Instron universal testing machine (model 8800) with a crosshead speed of 2mm/min and a load cell of 10 kN. The tensile testing was performed according to the ISO 527 standard for tensile testing on composites and plastics. At least six specimens were tested for each composition, and the results are presented as an average for tested samples.

TABLE II
Compositions of the Studied Composites

Materials	Matrix (wt %)	Filler (wt %)
PLA	100	0
PLA/MCC10	90	10
PLA/MCC15	85	15
PLA/MCC20	80	20
PLA/MCC25	75	25
PLA/WP25	75	25
PLA/WF25	75	25

Dynamic mechanical thermal analysis

Dynamic Mechanical Thermal Analysis (DMTA) was conducted using a Rheometrics Scientific V, to study the tan δ temperature and dynamic modulus of different composite systems. DMTA was run in a dual cantilever bending mode with typical sample dimensions: thickness 4mm, length 30mm, and width 10mm. Heating rate was 1.5°C/min, strain rate was 1mm/s, and frequency was 1 Hz.

Crystallinity studies (WAXD)

Wide angled X-ray diffraction (with a Siemens Diffractometer D5000) was used to study the crystallinity of the pure components and MCC composites. The samples were exposed for a period of 1.5 s for each angle of incidence (θ) using a Cu Kα X-ray source with a wavelength (λ) of 1.541E. The angle of incidence is varied from 4 to 50 by steps of 0.02s. The periodical distances (d) of the main peaks were calculated according to Bragg's equation ($\lambda = 2$ days sin θ).

Biodegradation studies

Biodegradability of pure PLA and the composites was studied at 58°C according to the ASTM D5338 standard. The water content of the soil was around 60% by weight. The compost used was of garden waste and supplied by Trondheim commune. Further, the soil was used as obtained and had no special microbial activity. The test specimens were compression molded to 2mm thickness, and the sample dimensions were approximately 6×6 cm^2. The samples were recovered from the soil at different stages of degradation and washed with distilled water, dried in the oven at 50°C, and weighed. Photographs of the samples were also taken for visual comparison.

RESULTS AND DISCUSSION

Morphology

The overview and detailed appearance of the used MCC is shown in Figure 2. It can be seen from the figure that the MCC is in particulate form and the

particle dimensions are in the range of 10–15 μm, having an aspect ratio (1/d) around 1 [(Fig. 2(b)]. It can also be seen that the MCC exists as aggregates of crystalline cellulose entities. It is also possible to see some nano fibrils on the MCC particle surfaces, which might be evidence that the MCC particles are agglomerates of hundreds of individual cellulose nano fibrils. Figure 3 shows the appearance of wood pulp and wood flour. Figure 3(a) shows wood pulp fibers (WP), which are in the form of single fibers having a size around 20 μm in diameter and 3500 μm in length. The detailed view of WP is a single fiber with highest aspect ratio (1/d = 175). Figure 3(b) shows WF, which is in the form of wood fiber bundles with dimensions ranging between 200 and 400 μm in diameter and 1000–1500 μm in length, giving a 1/d around 10.

The fracture surfaces of the composite specimens were studied to understand the failure mechanisms and also study possible interaction between different components. The fracture surfaces of PLA/MCC composites are given in Figure 4. Figure 4(a) is an overview of PLA/MCC composites showing a uniform dispersion of MCC in the PLA matrix. Another observation is that the MCC still remains as aggregates of crystalline fibrils and no separation had taken place during the extrusion process. Further in Figure 4(a), a large number of holes in the PLA matrix are visible

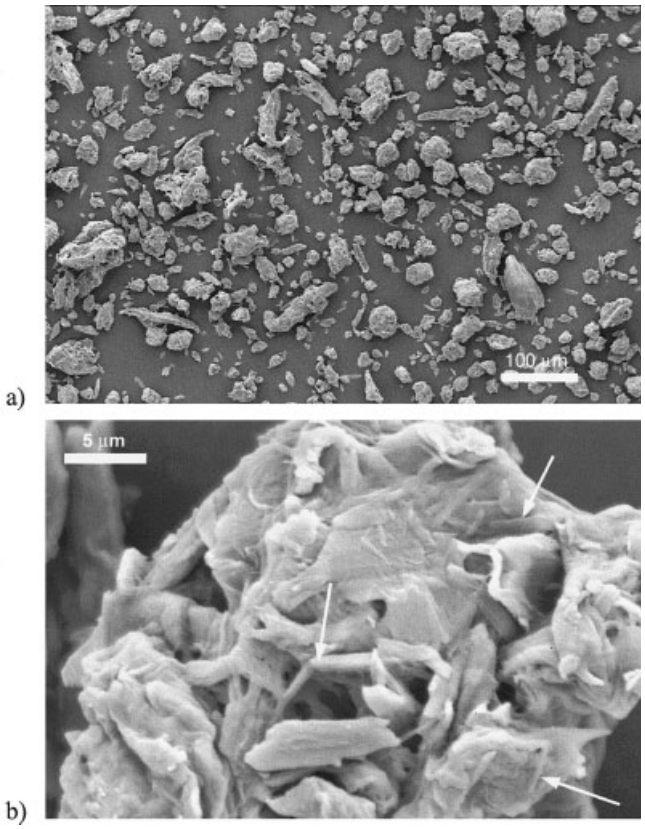

Figure 2 Structure and appearance of MCC: a) overview; and b) detailed view.

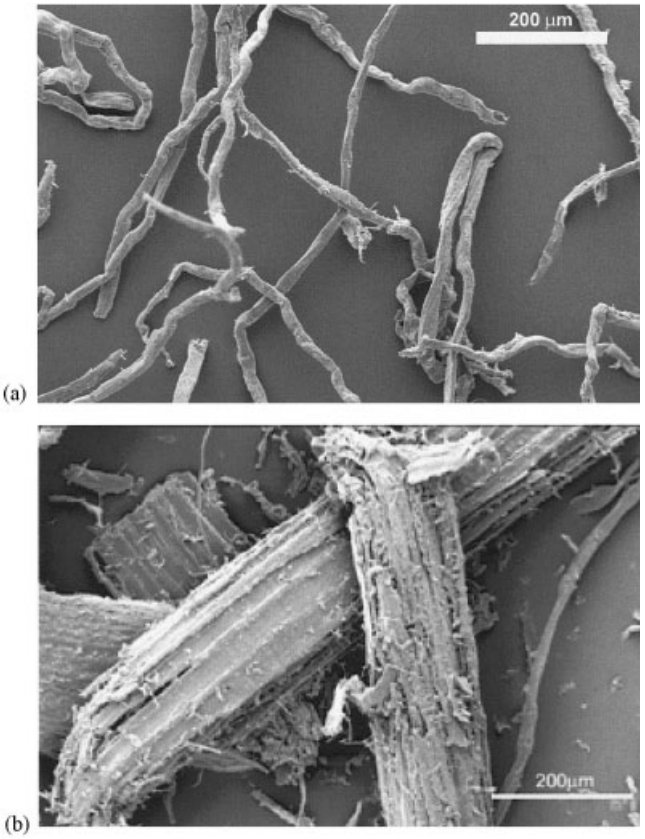

Figure 3 Morphology of used a) wood pulp, and b) wood flour.

where MCC have been located before the fracture. Figure 4(b), a more detailed micrograph, shows that there are voids around the MCC aggregates. Both observations, voids around the MCC and many holes in the matrix, indicate that there is no adhesion between the PLA and MCC.

Figure 5 shows the fracture surface of PLA/WP and PLA/WF composites. Figure 5(a) shows wood pulp composite. It is possible to see that wood pulp remains as single wood fibers with excellent dispersibility, which is not usually the case when wood pulp is blended with polyolefins.[29] This could be due to a specific interaction between the polyester matrix and cellulose. Gatenholm and coworkers have made similar conclusions in an earlier study of PHB-based cellulose composites.[30] Further observations in Figure 5(a) are that the single wood fiber surfaces are clean and it is also possible to see fiber pullouts. These observations indicate that there is no chemical adhesion with the PLA matrix, but if compared to Figure 4, PLA/MCC composites, the interaction is better. Figure 5(b) shows a wood flour composite. The first observation is that the wood fiber bundles are larger than the MCC and WP. The second observation, which was made during the SEM, is that it was difficult to identify the wood fibers from the PLA matrix; this is

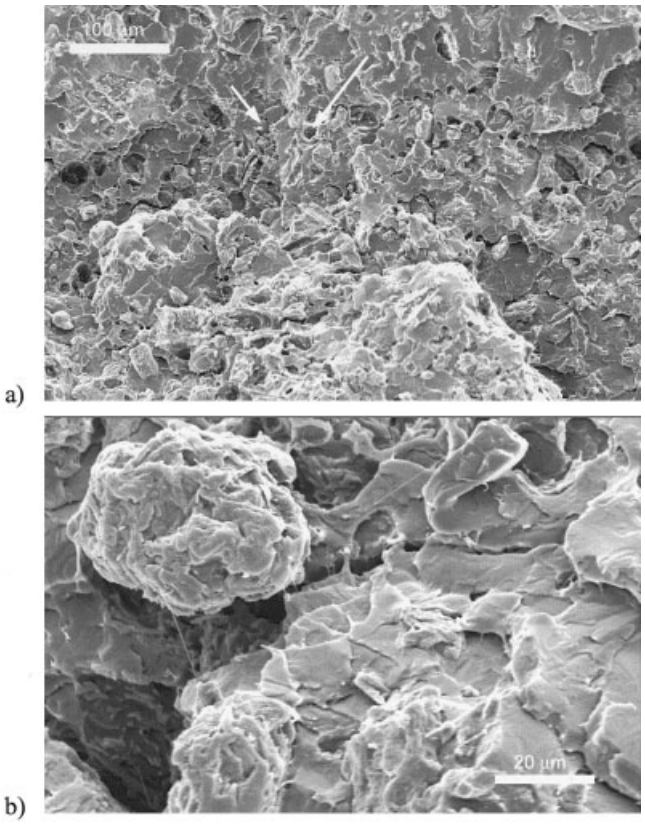

Figure 4 Microstructure of PLA/MCC composites: a) overview of PLA/MCC10, and b) detailed view of PLA/MCC25.

usually the case when there is good adhesion between the matrix and fibers because the fibers are coated with the polymer. In this case, it was not possible to obtain coated wood fibers but we believe that the mechanical interlocking is better in this system because of the roughness of the wood flour and that might contribute to improved adhesion.

Mechanical properties

Table III summarizes the mean and standard deviations of the mechanical properties of PLA and PLA composites. The results are also presented in more detail in separate figures.

Figure 6 shows typical tensile curves for pure PLA and PLA composites with different MCC content. The figure clearly shows that both tensile stress and elongation to break are lower for the composites compared to pure PLA and that the composites have slightly better stiffness compared to pure PLA. Figure 7 shows the modulus and tensile strength as a function of MCC content. It is clearly shown that increased MCC content has a negative effect on composites strength compared to pure PLA, while the modulus is slightly increased with increased MCC content. As the standard deviations of strength values are within the limits of differences, therefore, we can conclude that the strength remains almost constant between 10 to 25% MCC content.

Figure 8 shows typical tensile curves of pure PLA and composites with 25% of WF, WP, and MCC respectively. The tensile strength is again higher for pure PLA compared to the composites, but the strength is better for both WF and WP composites than for MCC composite. The elongation to break decreases again in the composites compared to the pure PLA, being in the order WP > WF > MCC.

Figure 9 compares the tensile strength and the modulus of composites with MCC25, WF25, and WP25 with pure PLA. All the studied composites have tensile modulus higher than pure PLA, and the WF system has highest modulus, followed by WP and then MCC. However, in this case, WF and WP can be considered to have the same modulus statistically, taking the standard deviations into consideration. The conclusion of the mechanical testing is that all composites have higher modulus than pure PLA but the incorporation of both WF and WP increases the modulus more than MCC does.

PLA is a brittle polymer, and it seems that the brittleness even increases with the addition of cellulose reinforcements. The elongation to break, for all

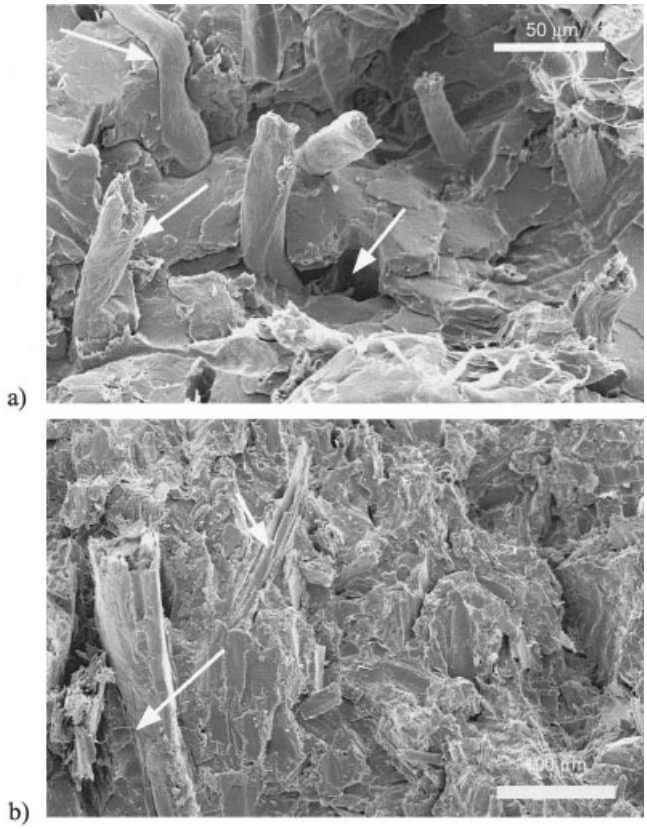

Figure 5 Microstructure of a) PLA/WP25 and b) PLA/WF25 composites.

TABLE III
Mechanical Properties PLA and Its Composites

Materials	Tensile strength (MPa)		Elongation at break (%)		E-Modulus (GPa)	
PLA	49.6	± 1	2.4	± 0.1	3.6	± 0.2
PLA/MCC10	38.2	± 0.5	1.8	0	4.1	± 0.7
PLA/MCC15	37.8	± 0.8	1.9	± 0.2	4.4	± 0.2
PLA/MCC20	38.1	± 0.7	1.8	± 0.1	4.7	± 0.3
PLA/MCC25	36.2	± 0.9	1.7	± 0.2	5.0	± 0.2
PLA/WP25	45.2	± 1.3	1.9	± 0.3	6.0	± 0.7
PLA/WF25	45.2	± 1.3	1.7	± 0.1	6.3	± 0.2

composites, is lower than that for pure PLA. The lowering of elongation to break with the addition of fibers to polymers is a common trend observed in thermoplastic composites.[31,32] When the three cellulose samples are compared, the elongation is the highest for the PLA/WP system followed by the PLA/WF system and is lowest for the PLA/MCC system. As the SEM study of composite microstructure showed, the WP was acting as single fibers with higher l/d ratio than WF or MCC and many fiber pullouts could be observed. Another observation made on WP composites was that wood pulp fibers seem to be soft (twisted and curled). Soft and longer fibers and fiber pullouts might result in better toughness and, therefore, also better elongation to break. The results might indicate that both WP and WF act better as reinforcements compared to MCC.

The mechanical performance of composites is expected to depend on the following factors: 1) adhesion between the PLA matrix and cellulosic reinforcements, stress transfer efficiency of the interface; 2) volume fraction of the fibers; 3) aspect ratio of the reinforcements; 4) fiber orientation; and 5) the degree of crystallinity of the matrix.[33]

The decrease in strength is an indication of poor stress transfer across the interphase, which means that there is practically no interfacial bonding between the reinforcing fiber and the polymer matrix.[34] The poor adhesion between the matrix and fiber initiates numerous voids at the fiber matrix interface, and the stress transfer to the fibers, which are the load bearing entities, becomes inefficient leading to low strength values.[35]

The higher tensile strength, elongation, and modulus of WP and WF systems can be explained based on the aspect ratio of the three reinforcements. The WP and WF have higher aspect ratio than MCC and that could enhance the mechanical performances even in the case when the adhesion is poor. This enhancement would occur in the case if the fiber length were equal to or higher than the critical fiber length, Lc. It is possible to see from the fracture surfaces in Figures 4 and 5 that there are debonding and fiber pullouts in all composite systems, which means that the fiber length is lower than the critical fiber length. In the case of MCC, which is a particulate reinforcement, the L $\ll$ Lc and, therefore, it is possible to obtain many debonded sites on the fracture surface. The low efficiency of stress transfer by particulate reinforcements in composites has been reported earlier.[36,37] The low aspect ratio and particulate nature leads to low elon-

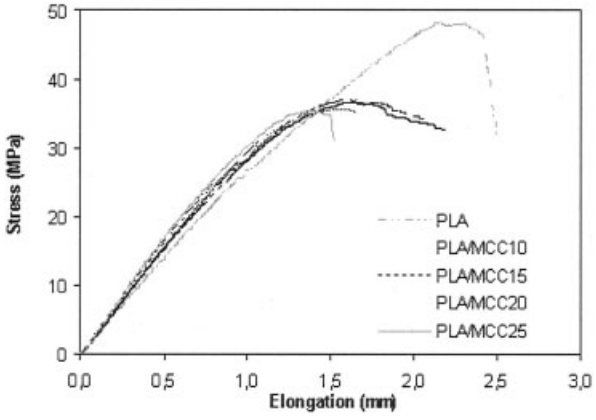

Figure 6 Typical tensile curves for PLA and PLA/MCC composites with different MCC contents.

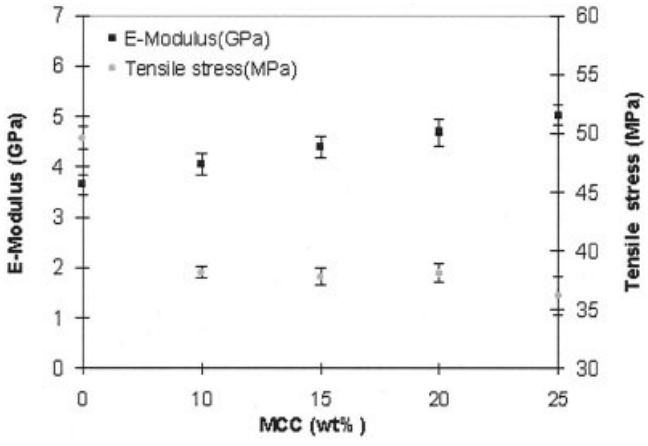

Figure 7 Stiffness and strength as a function of MCC content.

gation at break and brittleness. The high interfacial area is the only favorable aspect in the case of MCC and, therefore, the MCC system has mechanical properties comparable with wood pulp fiber (WP) and wood fiber (WF) systems in spite of its particulate nature.

The PLA is a semicrystalline polymer, and it is predicted that the crystallinity of the PLA will increase with the addition of cellulosic reinforcements. These crystalline regions then could act as physical crosslinks or filler particles, which could subsequently increase the modulus substantially. The higher modulus of the composites compared to pure PLA might be an indication that the crystallinity is higher for composites. However, during the fabrication of the composites, the cooling rate is fast, it is considered that the matrix is mostly amorphous, and the crystallinity may be primarily due to transcrystallinity of the PLA on the fiber surface. In addition, MCC has the highest surface area, which means that we would expect the highest transcrystallinity in the PLA/MCC system. However, the crystallinity in the system requires more detailed study, and the effect of crystallinity on composite properties will be reported in our forthcoming article in detail.

Dynamic mechanical thermal analysis

The DMTA of PLA/MCC composites was performed to investigate if the addition of the MCC would improve the thermal properties, such as maximum use temperature, for PLA. Five materials, PLA, PLA/MCC10, PLA/MCC15, PLA/MCC20, and PLA/MCC25, were tested to find the maximum use temperature and also to see the possible interaction between the PLA matrix and MCC. Figure 10 shows how the addition of different contents of MCC influenced the tan delta and dynamic modulus of PLA. Figure 10(a)

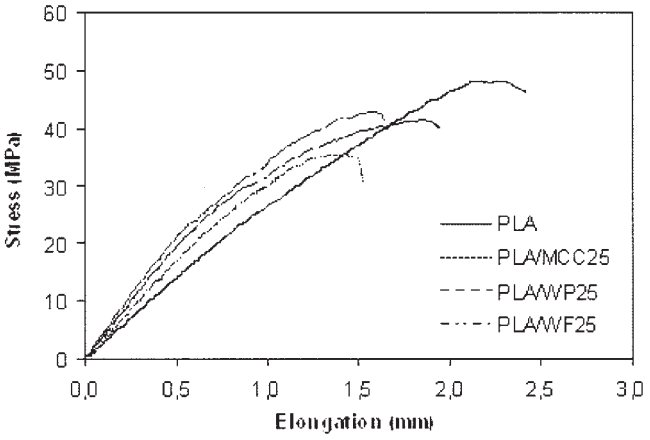

Figure 8 Tensile curves of pure PLA, and composites with 25% of wood flour, wood pulp, and MCC, respectively.

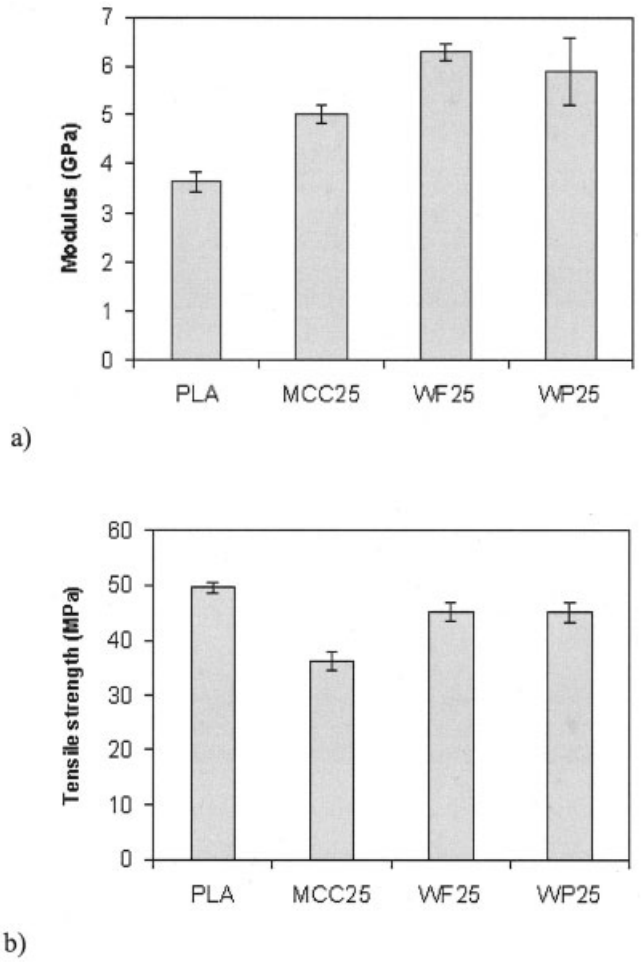

Figure 9 Comparison of the mechanical properties of PLA and its composites: a) tensile modulus, and b) tensile strength.

shows the effect of MCC content on the tan delta peak. It is possible to see that the tan delta peak (α-transition) is slightly shifted to higher temperature with increased MCC content. The shift to higher temperature usually indicates restricted molecule movement because of improved interaction in filled polymers.[38] The α-relaxation involves the movement of amorphous chains, and the presence of reinforcements and/or crystalline regions can act as physical crosslinks, decreasing the mobility of the amorphous regions and increasing the modulus.[35,33] The tan-delta peak of PLA was measured to be approximately at 67°C and that was increased to 69°C for MCC composites. However, in this case, the shift is not significant enough to indicate a strong interaction between the PLA and the MCC, which was also indicated by SEM study of this composite system. The dynamic modulus curves for composites with different MCC content are given in Figure 10(b). The modulus is almost the same for all the systems until the softening temperature. It could be noted that the addition of

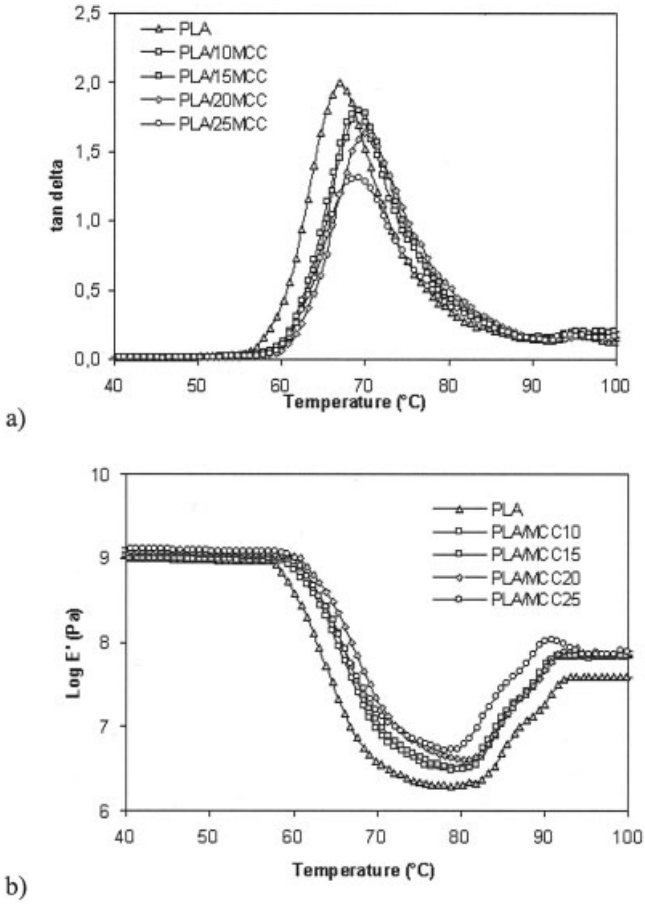

Figure 10 DMTA curves for PLA/MCC composites: a) tan delta, and b) dynamic modulus.

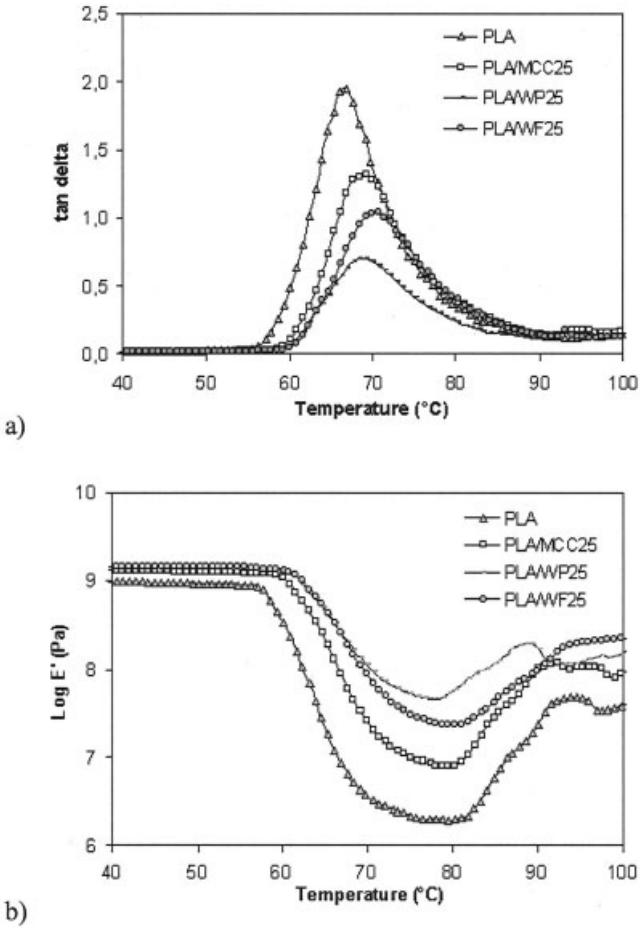

Figure 11 DMTA curves for PLA, PLA/MCC25, PLA/WF25, and PLA/WP25 composites: a) tan delta, and b) dynamic modulus.

MCC in PLA increased the softening temperature from 57 to 60°C. Further, it can be seen that around 80–90°C, the modulus increases again. This could be attributed to the cold crystallization of the semicrystalline PLA matrix, which is in conformity with the work carried out earlier.[26]

The values of glassy and rubbery modulus obtained from DMTA are given in Table IV. The rubbery modulus is obtained from the modulus values in the temperature range of 70–80°C, which is after the polymer relaxation and before the onset of cold crystallization. Above 80°C, the cold crystallization takes over and the modulus is governed by the crystallinity of the matrix. The rubbery modulus of MCC composites (at 75°C) is higher than that of PLA and it increases with MCC content. The rubbery modulus is known to depend on the crystallinity of the system, aspect ratio, and interaction between the phases. In the case of MCC composites, the adhesion and interaction between the phases was found to be poor and the aspect ratio is too low to have any significant effect on modulus. We expect that the MCC would act as a nucleating agent in PLA, and during cooling a transcrystalline layer of PLA on the MCC surface would be developed. This phenomenon might be correlated to the higher dynamic modulus observed in MCC composites. However, detailed study of the nucleating capability of MCC and the transcrystallization of PLA is required to confirm this assumption and will be discussed in detail in our next article.

Figure 11 shows the DMTA curves for PLA, PLA/

TABLE IV
The Effect of Cellulose Based Reinforcements on the Dynamic Modulus

	Dynamic modulus	
Materials	Glassy stage (10^8 Pa)	Rubbery stage (10^6 Pa)
PLA	6.4	2.15
PLA/MCC10	10.1	3.35
PLA/MCC15	10.9	3.53
PLA/MCC20	10.9	5.71
PLA/MCC25	10.4	8.45
PLA/WP25	11.9	46.7
PLA/WF25	13.1	24.5

25MCC, PLA/25WF, and PLA/25WP. Figure 11(a) shows the tan-delta peaks of PLA and composites with 25% of MCC, WP, and WF. The DMTA results indicate that the composites have a higher thermal stability compared to pure PLA. It was found that the α-transition for pure PLA is around 67°C and increases to 70°C for WF and 69.1°C in the case of WP and MCC. This can be explained based on the retardation in the relaxation of amorphous regions due to the physical interaction with the reinforcing phase and the crystalline regions of the matrix. Figure 11(b) shows the storage modulus curve of PLA and the composites. The composites exhibit an improvement in dynamic storage modulus and heat distortion temperature compared to pure PLA. The storage modulus values for glassy and rubbery are given in Table IV. The rubbery modulus (between 70 and 80°C) is higher for the composites than for pure PLA and is highest for WP fibers followed by WF and then MCC. When the three cellulose systems are compared, it can be seen that the increase in rubbery modulus is in direct correlation with the aspect ratio. Therefore, the aspect ratio can be considered as the governing factor in the relaxed modulus of the composites. The curves show a decrease on modulus at around 60°C, which indicates that the modulus increases again, which is a typical effect of cold crystallization. As the adhesion between the phases is poor in all the systems, this effect depends on aspect ratio of the reinforcement as well as crystallinity of the matrix.

These DMTA results lead to the conclusion that a small improvement in thermal stability is obtained by the addition of cellulosic reinforcements to the PLA matrix. The modulus also showed some improvement but not significant enough to indicate good interaction or adhesion between the phases. Therefore, the performance can be improved by enhancing the interaction between the matrix and reinforcement by adding compatibilizers, functionalizing the reinforcement or adding nano-sized reinforcements.

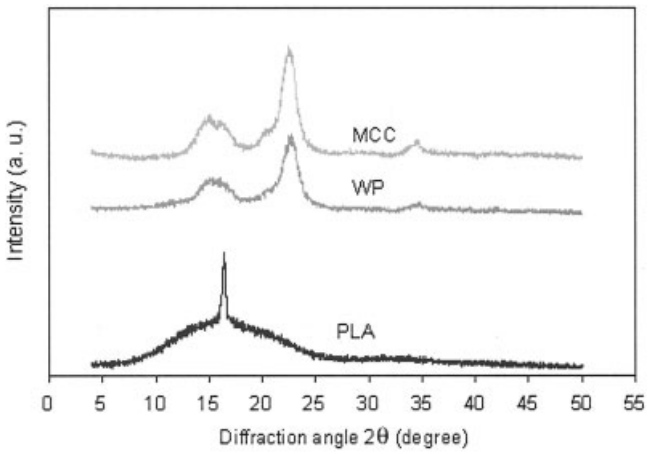

Figure 12 WAXD curves for raw materials used.

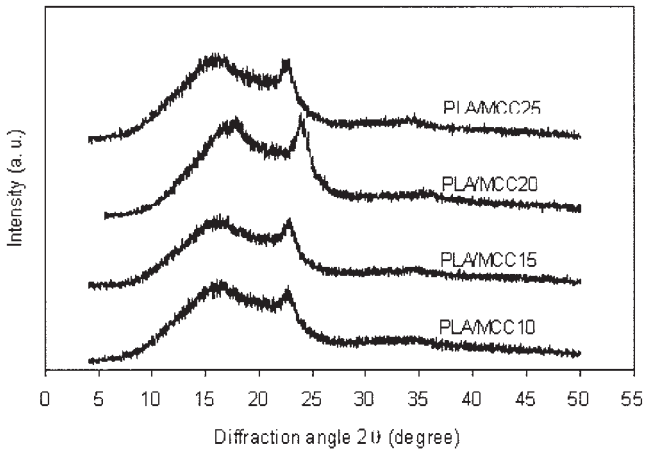

Figure 13 Diffraction pattern for PLA/MCC composites.

Wide angled X-ray scattering

The pure polymer and fiber components and composites were characterized by X-ray diffraction to study the effect of the type of reinforcement and MCC content on the crystallinity of PLA. The X-ray diffraction patterns for PLA, WP, and MCC are shown in Figure 12. In the figure, the WAXS pattern of wood fibers is not shown due to the difficulty in testing coarse wood flour.

Except for a narrow peak at $2\theta = 16.4$, PLA exhibits an amorphous nature and it can be considered as in a semicrystalline phase. The WP and MCC show peaks at $2\theta = 22.5$ and 34.5. In the case of MCC, additional peaks are seen at $2\theta = 15.4$ and 16.2 whereas in the case of wood pulp fibers, these peaks are not sharp and a shoulder is observed around the region $2\theta = 14$ to 17. The peaks are more prominent and sharp for MCC, showing the crystalline nature of this reinforcement. The d values associated with $2\theta = 15.4$, 16.2, 22.5, and 34.5 are 6.14, 5.46, 3.95, and 2.59 Å, which is corresponding to the cellulose I polymorph structure. Other scientists have reported the same results for MCC from X-ray analysis earlier.[37,38] Young and coworkers have concluded that high crystalline MCC is required for high performance composites with MCC. The wood pulp also shows peaks corresponding to the Cellulose I structure, but they are weaker and less prominent, indicating lower crystallinity. It is possible that wood pulp contains some residual lignin and that contributes to the slightly lower crystallinity of this fiber compared to that of MCC.

In Figure 13, the effect of MCC content on crystallinity of the system is shown. The peaks at $2\theta = 16.5$ and 22.6 are the most prominent and is indicative of PLA and cellulose crystallinity, respectively. As the MCC content increases to 25%, a steady increase in the intensity of the peaks at $2\theta = 22.6$ is observed. The peaks at $2\theta = 15.2$ and 16.3 are not prominent at low

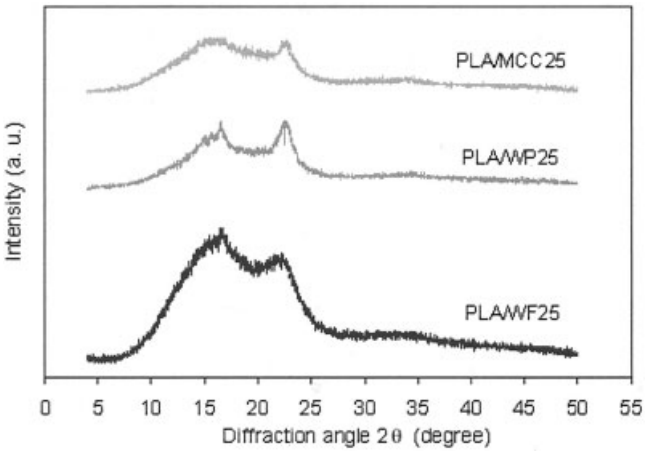

Figure 14 Comparison of crystallinity of PLA/MCC25, PLA/WF25, and PLA/WP25 composites using WAXD.

reinforcement content, and they are replaced by a broad shoulder around $2\theta = 16$, which indicates a more predominant amorphous material. For MCC composites, the XRD data is indicative of very low PLA crystallinity and the peaks due to PLA and cellulose-I are weak. The low intensity of the PLA peak is possibly explained by a low level of matrix crystallinity developed due to fast cooling rates during extrusion and injection molding.

In Figure 14 diffractograms of PLA and composites with 25% of WF, WP, and MCC are given. It can be seen that all the composites have weak crystalline bands and are mainly amorphous in nature, which can be due to the fast cooling during composite preparation. However, further study is necessary to confirm this effect. In the WF composite, a low intensity peak is observed at $2\theta = 16.7$ corresponding to PLA and a shoulder like hump is observed at $2\theta = 22.4$, which is indicative of low crystallinity of WF. In the case of the WP system, the peak is observed at $2\theta = 16.7$, corresponding to PLA. The peak at $2\theta = 22.7$ from the cellulose-I is also present in the composite. However, the peak at $2\theta = 15.4$ and 16.2 is not identifiable, and the system as a whole appears to have very low crystallinity. The MCC system has a low intensity peak at 22.7 from cellulose. In addition to this, a shoulder is visible around $2\theta = 15.8$ and 16.6, which originates from cellulose and PLA crystallinity. The MCC composite shows low PLA crystallinity compared to wood and pulp fiber composites, which is in agreement with the DMTA results. Therefore, it can be inferred that the PLA/WF and PLA/WP systems have a higher level of matrix crystallinity than the PLA/MCC system. This explains the lower modulus of the MCC system compared to the WF and WP systems.

In all cases, it can be seen that the magnitude of the peaks indicating crystallinity of the composite is lower than that of PLA and the reinforcement used. This probably results from the intermixing with PLA and also the random orientation of the reinforcement. The reinforcement is having a random arrangement, and the resultant crystallinity is expected to be less than the case when the reinforcement is oriented in a plane. This type of observation was reported by Dufresne and coworkers while working with tunicin whiskers filled composites.[39]

Biodegradability

Figure 15 shows the picture of samples recovered from compost soil at different stages of degradation. When biodegradable applications are considered, composting is the most preferred disposal route. The rate of hydrolytic degradation of PLA is dependent on temperature and the humidity level. In an environment of high humidity and a temperature of around 58 ± 2°C, PLA polymers were found to degrade rapidly.[40,41] Therefore, for the present study, temperature was maintained at ~ 58°C and moisture content of the soil was ~ 60%. In PLA degradation, moisture susceptibility is the primary driving force towards degradation and involves four steps, namely,. water absorption, ester cleavage forming oligomers, solubilization of oligomer fractions, and diffusion of soluble oligomers by bacteria.[42] It was found that the onset of PLA degradation occurred as early as 2 weeks and was marked by the embrittlement of the samples. The slower degradation rate in the composites is due to the resistance in water uptake and diffusion through the composite compared to pure PLA, which readily takes up water. However, the weight loss was not very significant for PLA or the composites until 8 weeks in compost soil. In Figure 16, the residual weight percentage (R_w %) of the composites as a function of time (in days) in compost soil is shown. It was seen that after 60 days in the compost soil, the composites also showed marked degradation. After 75 days, all the samples show a rapid increase in degradation, especially the WF composites. The figure shows that the WF composites have a higher rate of degradation than the WP and MCC composites. This leads to the conclusion that PLA/WF composites are more susceptible to water and thereby more biodegradable, compared to WP and MC composites.

CONCLUSIONS

This study was carried out as an initial step towards the use of microcrystalline cellulose (MCC) as reinforcement in the PLA matrix. The morphology studies of MCC particles showed that MCC exists as aggregates of nano-fibers/whiskers of cellulose. However, the morphology studies of the composites revealed the

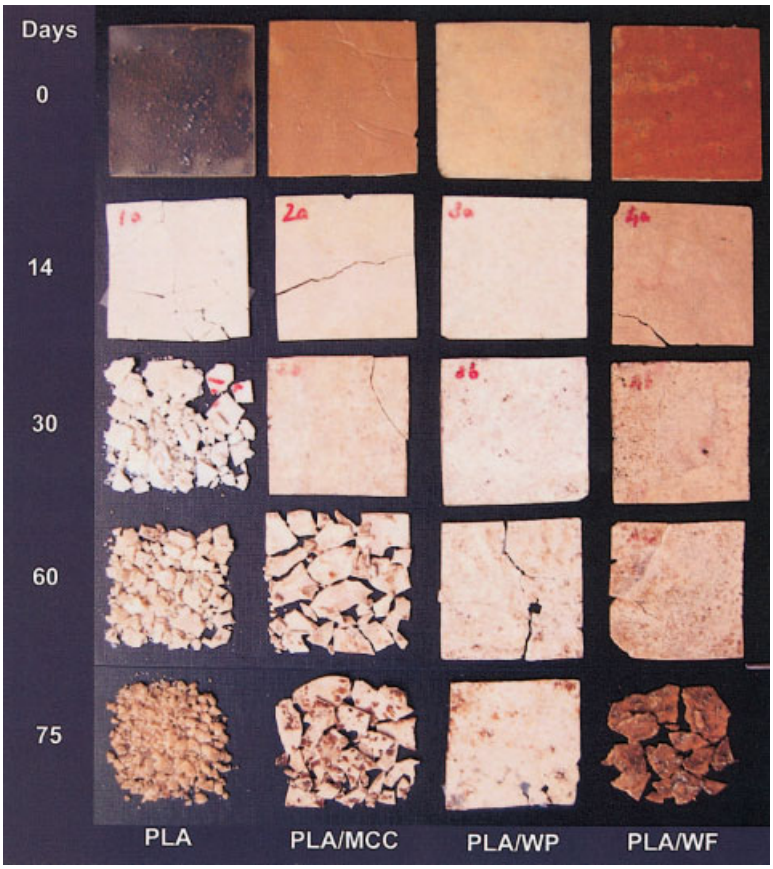

Figure 15 Photographs showing different stages of biodegradation of PLA and its composites in compost soil.

fact that the MCC did not separate into nano-whiskers during the extrusion process and remained as microparticles in the composite.

Further, the evaluation of the mechanical properties of the composites demonstrated that the tensile modulus was improved with increased MCC content, but tensile strength and elongation to break was decreased. It was also observed that both WF and WP resulted in composites with better mechanical properties compared to MCC composites, which may be due to poor interfacial adhesion between the phases as observed from SEM. Further, the morphology studies showed a good dispersion of all cellulose reinforcements in PLA, which depends on the nature of the polyester matrix.

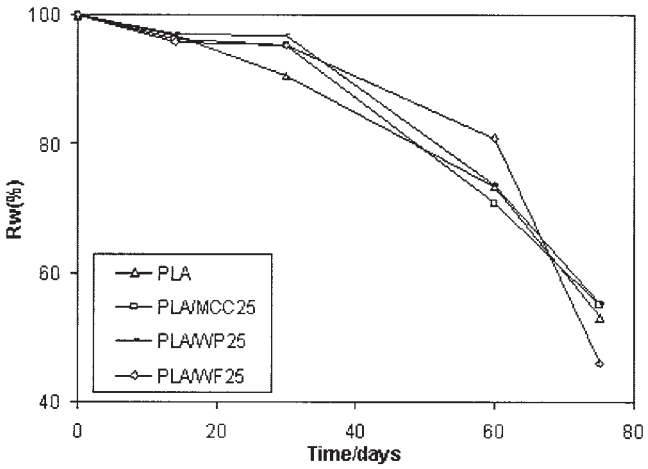

Figure 16 Residual w/o of PLA and its composites as a function of time in the compost soil.

DMTA studies showed that the storage modulus and thermal stability increased marginally with the addition of cellulosic reinforcement. The storage modulus of the composites changed in the order WP > WF > MCC > PLA. This change in storage modulus is predicted to be governed by the aspect ratio of cellulose reinforcements.

XRD studies showed that both MCC and wood pulp have cellulose-I structure but the crystallinity is higher for MCC than for wood pulp. The results also showed that PLA exhibited a single sharp peak and is semicrystalline in nature. All composites showed lower crystallinity than the pure component phases. The higher crystallinity of PLA in WP and WF composites compared to MCC composites can be considered as one of the possible reasons for the better mechanical performance of WF and WP composites compared to MCC composites.

Biodegradation studies on the composites showed that PLA started degrading by 3–4 weeks while the composites started degrading rapidly during 4–8 weeks. The degradation rate was found to be higher for WF composites than for MCC and WP composites. We believe that the incorporation of MCC in PLA after separation into nano-whiskers will result in high performance biodegradable composites.

The authors thank Fortum Oil and Gas Oy, Finland, Borregaard Chemcell, Norway, Scandinavian Wood Fiber AB, Sweden, and Rayonier, USA, for supplying the materials.

References

1. Aurich, T.; Mennig, G. Polym Compos 2001, 22, 680.
2. Hornsby, P. R.; Hinrichsen, E.; Tarverdi, K. J Mater Sci 1997, 32, 1009.
3. Gassan, J.; Bledzki, A. K. Compos A 1997, 28A, 1001.
4. Joseph, P. V.; Joseph, K.; Thomas, S. Compos Sci Technol 1999, 59, 1625.
5. Oksman, K. Appl Comp Mat 2000, 20, 403.
6. Bledzki, K.; Gassan, J. Prog Polym Sci 1999, 24, 221.
7. Corbie're-Nicollier, T.; Laban, B. G.; Lundquist, L.; Leterrier, Y.; Manson, J.-A. E.; Jolliet, O. Resour Conserv Recycl 2001, 33, 267.
8. Zafeiropoulosa, N. E.; Williamsb, D. R.; Bailliea, C. A.; Matthewsa, F. L. Compos A 2002, 33, 1083.
9. Sathyanarayana, K. G.; Sukumaran, K.; Mukherjee, P. S.; Pavithran, C.; Pillai, S. G. K. Cement and Concrete Composites 1990, 12, 117.
10. Paul, M. A.; Alexandre, M.; Degee, P.; Henrist, C.; Rulmont, A.; Dubois, P. Polymer 2003, 44, 443.
11. Mathew, A. P.; Dufresne, A. Biomacromol 2002, 3, 609.
12. Williams, G. I.; Wool, R. P. Appl Comp Mat 2000, 7, 421.
13. Oksman, K.; Selin, J.-F. In Natural Fibers, Plastics and Composites; Wallenberger, F. T.; Weston, N. E., Eds.; Kluwer Academic Publishers: Dordrecht/Boston/London, 2004; pp 149–165.
14. Mishra, S.; Tripathy, S. S.; Mishra, M.; Mohanty, A. K.; Nayak, S. K. J Reinforced Plastics and Composites 2002, 21, 5570.
15. Kalaprasad, G.; Joseph, K.; Thomas, S. J Mater Sci 1997, 59, 4260.
16. Paul, A.; Thomas, S. J Appl Polym Sci 1997, 63, 247.
17. Felix, J. M.; Gatenholm, P. J Appl Polym Sci 1991, 42, 609.
18. Oksman, K. Wood Sci and Technol 1996, 30, 197.
19. Dufresne, A. Recent Developments in Macromolecular Res 1998, 3, 455.
20. Mattoso, L. H. C; Ferreira, F. C.; Curvelo, A. A. S. In Lignocellulosic-Plastic Composites; Leao, A. L.; Carvalho, F. X.; Frollini, E., Eds; SINC do Brazil Tepperman: Sao Paulo, Brazil, 1997; p 241.
21. Periera, N.; Sousa, M. L.; Agnelli, J. A. M.; Mattoso, L. H. C. Effect of Processing on the Properties of Polypropylene Reinforced with Short Sisal Fibers; 4th Int Conf Wood Fiber Plastic Composites, Madison, WI, USA, May 12–14, 1997; p 206.
22. Osman, M. A.; Atallah, A.; Müller, M.; Suter, U. W. Polymer 2001, 42, 6545.
23. Schadler, L. S.; Giannaris, S. C.; Ajayan, P. M. Appl Phys Lett 1998, 73, 3842.
24. Kasuga, T.; Ota, Y.; Nogami, M.; Abe, Y. Biomaterials 2001, 22, 19.
25. Lee, J. H.; Park, T. G.; Park, H. S.; Lee, D. S.; Lee, Y. K.; Yoon, S. C.; Nam, J. Biomaterials 2003, 24, 2773.
26. Oksman, K.; Skrifvars, M.; Selin, J.-F. Compos Sci Technol 2003, 63, 1317.
27. Hamad, W. Cellulosic Materials: Fibers, Networks and Composites; Kluwer Academic Publishers: Boston, MA, 2002; p 47.
28. Eichhorn, S. J.; Baillie, C. A.; Zafeiropoulos, N.; Mwaikambo, L. Y.; Ansell, M. P.; Dufresne, A.; Entwistle, K. M.; Herrera-Franco, P. J.; Escamilla, G. C.; Groom, L.; Hughes, M.; Hill, C.; Rials, T. G.; Wild, P. M. J Mater Sci 2001, 36, 2107.
29. Felix, J.; Gatenholm, P. J Appl Polym Sci 1991, 52, 689.
30. Gatenholm, P.; Kubåt, J.; Mathiassin, A. J Appl Polym Sci 1992, 45, 1667.
31. Qui, W.; Zhang, F.; Endo, T.; Hirotsu, T. J Appl Polym Sci 2003, 87, 337.
32. Colom, X;. Carrasco, F.; Pages, P.; Canavate, J. Compos Sci Technol 2003, 63, 161.
33. Dufresne, A.; Dupeyre, D.; Paillet, M. J Appl Polym Sci 2003, 87, 1302.
34. McCrum, N. G.; Buckley, C. P.; Bucknall, B. In Principles of Polymer Engineering; Oxford University Press: New York, 1988.
35. Angles, M. N.; Salvado, J.; Dufresne, A. J Appl Polym Sci 1999, 74, 1962.
36. Cox, H. L. Br J Appl Phys 1952, 3, 72.
37. Eichhorn, S. J.; Young, R. J. Cellul 2001, 8, 197.
38. Averous, L.; Fringant, C.; Moro, L. Polymer 2001, 42, 6565.
39. Angles, M. N.; Dufresne, A. Macromol 2000, 33, 8344.
40. Lunt, J. Polym Degrad Stab 1998, 59, 14.
41. Ho, K. G.; Pometto III, A. L.; Hinz, P. N. J Environ Polym Degrad 1999, 7, 83.
42. Ray, S. S.; Yamada, K.; Okamoto, M.; Ueda, K. Nanoletters 2002, 2, 1093.